Originally published as:

Increased record-breaking precipitation events under global warming

Jascha Lehmann[*1,2]**, Dim Coumou**[1]**, Katja Frieler**[1]

[1]Potsdam Institute for Climate Impact Research, Germany

[2]University of Potsdam, Germany

*Corresponding author: J. Lehmann, jascha.lehmann@pik-potsdam.de, Telegrafenberg A26, 14473 Potsdam, Germany

Abstract.

In the last decade record-breaking rainfall events have occurred in many places around the world causing severe impacts to human society and the environment including agricultural losses and floodings. There is now medium confidence that human-induced greenhouse gases have contributed to changes in heavy precipitation events at the global scale. Here, we present the first analysis of record-breaking daily rainfall events using observational data. We show that over the last three decades the number of record-breaking events has significantly increased in the global mean. Globally, this increase has led to 12% more record-breaking rainfall events over 1981-2010 compared to those expected in stationary time series. The number of record-breaking rainfall events peaked in 2010 with an estimated 26% chance that a new rainfall record is due to long-term climate change. This increase in record-breaking rainfall is explained by a statistical model which accounts for the warming of air and associated increasing water holding capacity only. Our results suggest that whilst the number of rainfall record-breaking events can be related to natural multi-decadal variability over the period from 1901 to 1980, observed record-breaking rainfall events significantly increased afterwards consistent with rising temperatures.

1   Introduction:

The last decade has produced a large number of extreme weather events worldwide, including record-breaking rainfall events [*Coumou and Rahmstorf*, 2012]. The year 2010 has so far been the wettest year on record over land in terms of total precipitation [*NOAA National Climatic Data Center*, 2010], setting new record-breaking rainfall events on different time scales over many parts of the world [*Trenberth*, 2012]. This seeming accumulation of weather extremes in an exceptionally warm decade has raised the question of whether these events are related to climatic change.

A number of studies have addressed this issue using observational data sets and climate models [*Pall et al.*, 2007; *Zhang et al.*, 2007, 2013; *Min et al.*, 2011; *Shiu et al.*, 2012; *Benestad*, 2013; *Berg et al.*, 2013; *Singh and O'Gorman*, 2014]. The main finding is that over the recent past trends towards stronger precipitation extremes can be found over a larger fraction of the land area than trends towards weaker precipitation extremes [e.g. see references in *Seneviratne et al.*, 2012]. For example, Westra et al. [2013] found a significant increase in annual maximum daily precipitation extremes on a global scale.

Climate models suggest that the thermodynamic change in saturation vapor pressure as described by the Clausius-Clapeyron relation is a good predictor for changes in extreme rainfall intensities [*Pall et al.*, 2007]. This relationship predicts an increase in water vapor of typically 7% per degree of warming assuming constant relative humidity. However, dynamical changes can also influence the frequency and intensity of precipitation and thus disrupt the Clausius-Clapeyron expected change [*Trenberth*, 2011]. For example, changes in extratropical storm tracks will affect rainfall in mid-latitude regions [*Scaife et al.*, 2011; *Hawcroft et al.*, 2012]. The response of convective precipitation to warming can exceed the Clausius-Clapeyron rate [*Berg et al.*, 2013] which will have the strongest effects in the tropics.

Most studies used extreme value theory to analyze changes in threshold events, i.e. those exceeding a specified threshold of the climatological precipitation distribution [e.g., *Kharin et al.*, 2007; *Trenberth et al.*, 2007; *Min et al.*, 2011; *Westra et al.*, 2013]. This usually involves fitting an extreme value distribution to the tail of the observed distribution. However, small sample sizes in the tail result in unstable fits which can have strong affects on the results [*Frei and Schär*, 2001].

Here, we present the first global analysis of observed record-breaking daily precipitation events between 1901 and 2010 and how their frequency differs from that expected in a stationary climate. Analyzing record-breaking events has the advantage that no assumption on the underlying probability distribution function has to be made. This also implies that with this method no statements can be made about the exact changes in the underlying probability distribution in terms of shifts in the mean or higher order moments. However, here, we are interested in whether record-breaking rainfall events have increased or not, irrespective of the exact underlying changes in probability distribution. Thereby, the number of observed record-breaking rainfall events can be compared to the number expected in a climate with no long-term trend. This approach has been proven insightful for understanding the increase of heat extremes in a warming world [*Benestad*, 2003, 2004; *Redner and Petersen*, 2005; *Meehl et al.*, 2009; *Anderson and Kostinski*, 2011; *Coumou et al.*, 2013].

2 Data and Method

2.1 Data

We use monthly maximum 1-day precipitation data (Rx1day) from HadEX2 [*Donat et al.*, 2013b], a 3.75° x 2.5° gridded data set covering 1901-2010 (Fig. S1 in Supplementary Information (SI)). Globally aggregated quantities over land are dominated by the northern extratropics which account for roughly 2/3 of the total available data (Fig. 1, Fig. S2b). Spatial coverage varies over time with best coverage between 1960 and 2000 (Fig. S2a).

We analyze record-breaking events in each monthly Rx1day time series and subsequently take annual (12 calendar months) and boreal winter (Nov-Dec-Jan-Feb-Mar (NDJFM)) and summer (May-Jun-Jul-Aug-Sep (MJJAS)) averages. To ensure feasible statistics we restrict analysis to (1) time series with at least 30 years of data and (2) regions and time periods which had at least 100 non-missing values at each time slice. The maximum time period was found for which these criteria hold.

To test the robustness of our findings, we applied the analysis also to a second data set, the Global Historical Climatology Network (GHCNDEX) [*Donat et al.*, 2013a], which has a spatial resolution of 2.5° x 2.5° and covers 1951 – 2014. The spatial coverage is similar to that for HadEX2 (Fig. S3) and thus also the relative share of climatic zones to the global aggregate is roughly the same (Fig. S4). We repeated the analysis with HadEX2 for the time period
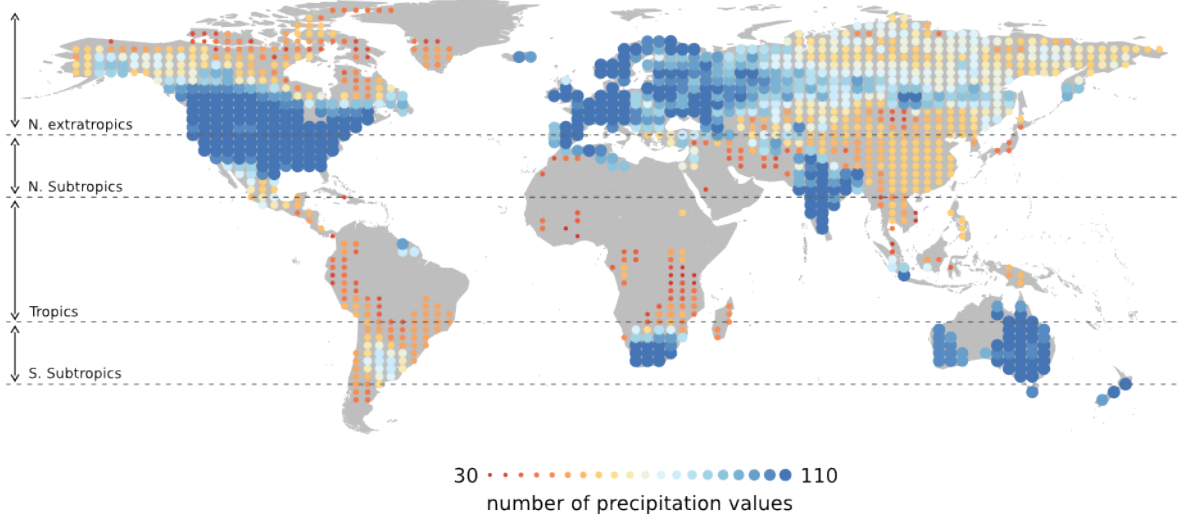
Fig. 1 Time series length of monthly maximum 1-day precipitation data covered at each grid point with a value of 110 indicating full coverage over 1901-2010. The magnitude is represented by the color and size of the dots.

1951-2010 to allow for a direct comparison of both data sets for the overlapping time period. In general, results are very similar between both data sets and thus confirm the robustness of our findings (see detailed description in SI, Fig. S5).

2.2 Observed versus iid-expected record-breaking events

A rainfall value (in mm) is defined as record-breaking if it exceeds all previous values in the given time series. Due to the sparseness of record-breaking events, it is difficult to make statements about climate change for a particular location only. We therefore aggregate the number of record-breaking events over seasons and regions as defined in Fig. 4 (see also table S1 in SI).

We assume that time series in a stationary climate can be described by independent and identically distributed (iid) values. For iid time series the number of expected record-breaking events at time N is equal to $\sum_{n=1}^{N} 1/n$. We normalize the number of observed record-breaking events with the analytical solution by defining the record-breaking anomaly:

$$R_{anom} = \frac{R_{obs} - R_{1/n}}{R_{1/n}} \cdot 100 \, (\%),$$

[1]

where R_{obs} is the sum of all observed record-breaking events in time series within a given region for a given time period and all calendar months of the given season. Analogously, $R_{1/n}$ is the analytically expected number of record-breaking events summed over the same region and time span. Thereby, missing values in the original time series are also accounted for in the calculation of $R_{1/n}$, respectively (see Fig. S6 for a schematic illustration). The null-hypothesis of a stationary climate thus accounts for the same spatial and temporal inhomogeneity as in the observations and hence for vacancies and the systematic increase of available data over time. An increase in observing sites will thus increase R_{obs} but also $R_{1/n}$ in the same way and therefore this will not lead to a bias in R_{anom}. By definition, the first value of each time series is always a record-breaking event and hence equal to the iid-expected value. To avoid this artificial start value of $R_{anom} = 0$ we start counting record-breaking events at the second time step.

To test whether the observed number of record-breaking events is significantly different from those in a stationary climate we create a distribution of simulated record-breaking events derived from iid time series. The iid assumption for the stationary model is justified because the detrended observational time series are close to iid (see S1: 'Testing iid assumption' in SI). The original month specific observational time series are shuffled (in the process of which any trend, change in variance, and autocorrelation is removed) to create a set of iid time series which are based on the original observational data.

This method has the advantage that no assumption on the parametric form of the underlying distribution is made. The spatial and temporal inhomogeneity of the observations had to be treated carefully. The number of observing sites systematically increased over time with some regions only providing observations after a certain time (Fig. 1 and Fig. S2). A limitation of our method is that for a set of time series one can either account for these inhomogeneities in the data availability over time (by "freezing" missing values during re-sampling) or for spatial correlation (by synchronous re-sampling) but not both at the same time. To overcome this, our method accounts for spatial correlation *within* regions and for data inhomogeneities *between* regions. The latter tends to be small within regions but can be large between regions (Fig. S8-S10), i.e. between for example Europe and Central Africa. The method thus accounts for these large-scale data inhomogeneities as shown by a similar increasing trend in data coverage in the shuffled data set as compared to observations (Fig. S8-S10). Spatial correlation on the other hand can be pronounced for nearby grid points and hence primarily within regions. Our

method is a balance to account for both effects when estimating confidence intervals, and it can be considered a conservative estimate (see sensitivity analysis later).

Time series within one region are shuffled in time using exactly the same re-sampling order such that the existing spatial correlation is maintained. Also to calculate seasonal aggregates the same re-sampling order is used for each monthly time series of the given season to account for possible correlations from one month to the next. The shuffling is repeated 10.000 times to create a distribution of record-breaking events under the Null hypothesis of the iid-model. The mean of this distribution follows the analytically expected number of record-breaking events in iid time series ($\sum_{n=1}^{N} 1/n$) and thus normalizing according to equation 1 provides a distribution centered around 0.

We define the observed record-breaking anomaly to be statistically significant if it is outside the 95% confidence range of this distribution of record-breaking anomalies calculated based on the shuffled time series.

To compute global mean statistics all grid points are separated into 21 smaller regions (see table S1) to which the shuffling is applied. Subsequently, all regional results are combined to come up with a global aggregate. Thus, the shuffling method accounts for changes in data coverage between regions which results in a suitable representation of temporal changes in global data coverage (Fig.S8-10).

Other studies which analyzed precipitation extremes have used a similar approach but shuffled fixed-sized blocks of 2-3 years to account for autocorrelation [*Kiktev et al.*, 2003, 2007; *Alexander et al.*, 2006]. The block size is derived from the variance inflation factor (*V*) which depends on the autocorrelation at all time lags and can thus be interpreted as a measure for the "time between effectively independent samples" [*Wilks*, 1997]. Similar to Westra et al. [2013], we find that due to little autocorrelation in our time series (we find a mean *V* of ~1.1) a block size greater than one is not necessary. We tested the sensitivity of our confidence intervals to different block sizes and found essentially no changes in confidence intervals (see Fig. S11-12). Further, we find that the confidence intervals for regional analyses decrease if we account for data inhomogeneity rather than spatial correlation within regions (compare Fig. 2 and Fig. S7). Thus, our confidence intervals can be considered as conservative and robust estimates.

6

Long-term non-linear trends in record-breaking anomaly time series are computed using singular spectrum analysis (ssa) with a window length of 15 years. This method uses eigenvalue decomposition to separate non-linear trends from white noise which gives similar results as a 30-yr moving average [*Allen*, 1997; *Golyandina et al.*, 2001].

2.3 Statistical Clausius-Clapeyron model

We further compare the number of observed record-breaking events to the expected number of record-breaking events assuming that the intensity of maximum daily precipitation increases with saturation vapor pressure according to the Clausius-Clapeyron equation. The Clausius-Clapeyron model consists of ensembles of precipitation time series which are composed of (1) a thermally induced long-term non-linear trend (pr_{therm}^{trend}) where precipitation changes are deterministically based on temperature using the Clausius-Clapeyron equation with (2) added stochastic year-to-year variability (Δpr) based upon the non-linearly detrended original precipitation time series:

$$pr = pr_{therm}^{trend} + \Delta pr . \qquad [2]$$

The thermally induced non-linear trend is calculated for each grid point and each month using

$$pr_{therm}^{trend} = \overline{pr} \cdot \delta pr_{therm}, \qquad [3]$$

where $\overline{pr}$ is the climatological mean of Rx1day time series over the full time period and

$$\delta pr_{therm} = \frac{e_s(\mathrm{T}^{trend}) - \overline{e}_s(\overline{\mathrm{T}})}{\overline{e}_s(\overline{\mathrm{T}})} \cdot 100 \qquad [4]$$

is a time series with changes in precipitation due to the changes in temperature, which arise from the difference between the temperature averaged over the full time period ($\overline{T}$) and the non-linear trend in temperature (T^{trend}). The change in precipitation is estimated by an approximation of the Clausius-Clapeyron equation

$$e_s(\mathrm{T}) = 6.1094 \cdot \exp\left(\frac{17.625T}{T + 243.04}\right). \qquad [5]$$

This statistical model thus assumes that extreme precipitation changes with temperature according to the potential of the atmosphere to hold more moisture at higher temperature. We used the CRU TS3.21 monthly temperature data [*Harris et al.*, 2014] taken from the Climate Research Unit (CRU), which provides absolute surface temperatures on a 0.5° x 0.5° grid. The record-breaking anomaly for the Clausius-Clapeyron is normalized using equation [1] and its confidence intervals are determined using the same shuffling method as for the iid model.

3   Record-breaking anomaly over time

3.1   Comparison between observed and iid-expected record-breaking events

On a global scale, the most prominent feature is a strong and consistent increase in the annual record-breaking anomaly since the 1980s as indicated by the long-term non-linear trend shown in Fig. 2a (black line). The record-breaking anomaly peaks in 2010, which saw +88% more record-breaking events (grey bars) than expected by the iid case. The long-term non-linear trend of the global record-breaking anomaly significantly increases from 1980 onward reaching +26% in 2010. A significant increase in the long-term non-linear trend between 1980 and 2010 is also seen over the northern extratropics (+31% in 2010) and in the tropics (+31% in 2010). The northern subtropics have also seen an upward trend but it is not statistically significant (+13% in 2010).

The long-term non-linear trend of the record-breaking anomaly shows multi-decadal variability which is most pronounced in the northern extratropics but also seen globally. Over the first 80 years the observed non-linear trend varies within the 95% confidence interval of the iid-model with the only exception of a short negative excursion around 1930 in the northern subtropics and the tropics. This coincides with a relatively warm period between 1920-1940 over the Northern Hemisphere [*Rogers*, 1985]. Note that the northern subtropics and the tropics were only coarsely sampled in the 1930s (Fig. 2a) so the negative excursion is likely a local phenomenon only. Due to the applied data requirements the sparse data coverage over the tropics only allows to compute the record-breaking anomaly for the 1901-1940 period if all calendar months are included but not for individual seasons.

During NDJFM, the evolution of the record-breaking anomaly is very similar to that for the annual results (Fig. 2f-j). However, during boreal winter, the year-to-year variability in the
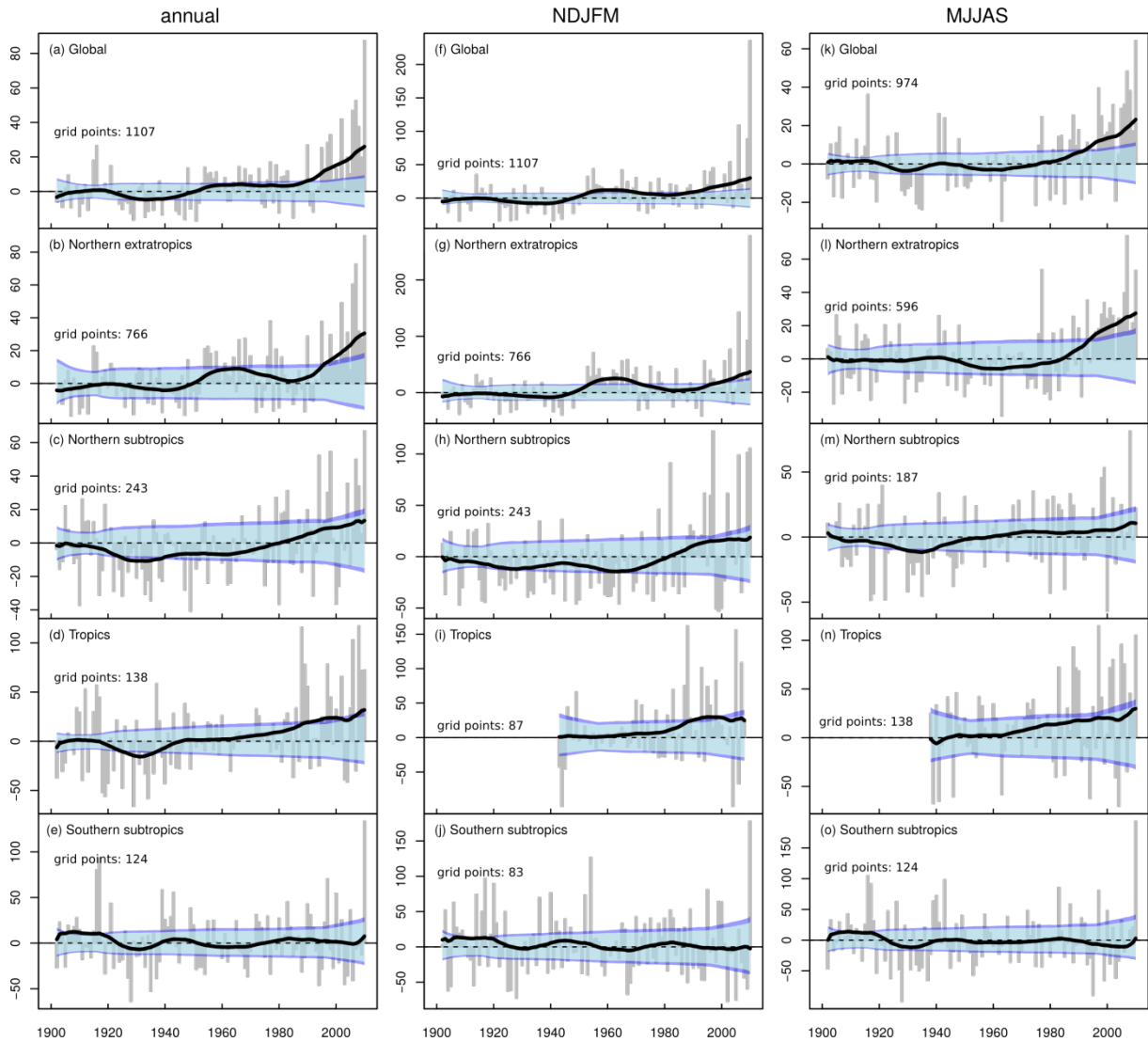
Fig. 2 Annual record-breaking anomaly (grey bars) shown (a) globally and for (b) northern extratropics, (c) northern subtropics, (d) tropics, and (e) southern subtropics. The long-term non-linear trend in record-breaking anomaly (black line) is calculated using singular spectrum analysis with window length of 15 years. The shaded areas reflect the 90% (light blue shading) and 95% (dark blue shading) confidence interval for equally computed long-term non-linear trends of the iid-model. The solid black line is thus directly comparable to the shaded confidence intervals. (f)-(j) and (k)-(o) are the same as (a)-(e), respectively, but for seasonal record-braking anomalies representing NDJFM (middle panel) and MJJAS (right panel).

number of record-breaking events in the northern extratropics and subtropics is generally larger compared to annual results. In addition, the increase in record-breaking anomaly over the Northern Hemisphere towards the end of the time series is stronger in NDJFM than in the annual mean. Specifically, the global record-breaking anomaly peaks in the 2010/11 winter

9

with a value of +230% (Fig. 2f). Also the observed long-term non-linear trend of the record-breaking anomaly during NDJFM is large reaching +30% (globally), +37% (northern extratropics), and +18% (northern subtropics) by 2010. In the tropics and southern subtropics the non-linear trend in record-breaking anomaly is similar in both seasons and in annual analysis.

During MJJAS (Fig. 2k-o), the year-to-year variability and the long-term non-linear trend of the record-breaking anomaly are similar to that of the full year (Fig. 2k, l). Nevertheless, whereas globally and over the northern extratropics the time series of the annual and boreal winter record-breaking anomaly show generally positive values between 1950-1980, the record-breaking anomaly during MJJAS remains negative. Over the northern subtropics this pattern inverts with negative anomalies in NDJFM and positive anomalies in MJJAS during 1950-1980.

Thus, globally and over the northern extratropics the increase in the long-term non-linear trend of record-breaking events towards the end of the 20th century is significant at the 5% confidence level in both summer and winter season (Fig. 2f, g and 2k, l).

3.2 Comparing trends in observed, iid-expected, and thermal induced record-breaking anomalies

The Clausius-Clapeyron model predicts an increase in annual record-breaking rainfall anomaly starting around 1970 for the northern extratropics, northern subtropics, and globally but little change in the tropics and southern subtropics (see Fig. 3.a-e). The model is able to capture the statistically significant increase of the observed long-term non-linear trend since the 1980s detected globally and over the northern extratropics and subtropics.

In the tropics, the Clausius-Clapeyron model predicts no change in contrast to a consistent (but not significant) increase in the observed record-breaking anomaly (Fig. 3d, i, n). In time series with a linear trend, the number of record-breaking events scales with the ratio of the magnitude of the linear trend to the short term variability [*Rahmstorf and Coumou*, 2011]. In the warm tropics, the absolute increase in thermal induced precipitation per degree of warming as described by equation [5] is larger compared to cooler regions. On the other hand, the short term variability in tropical time series is about four times larger than in the extratropics leading to a relatively small trend-to-variability ratio. As a consequence, the
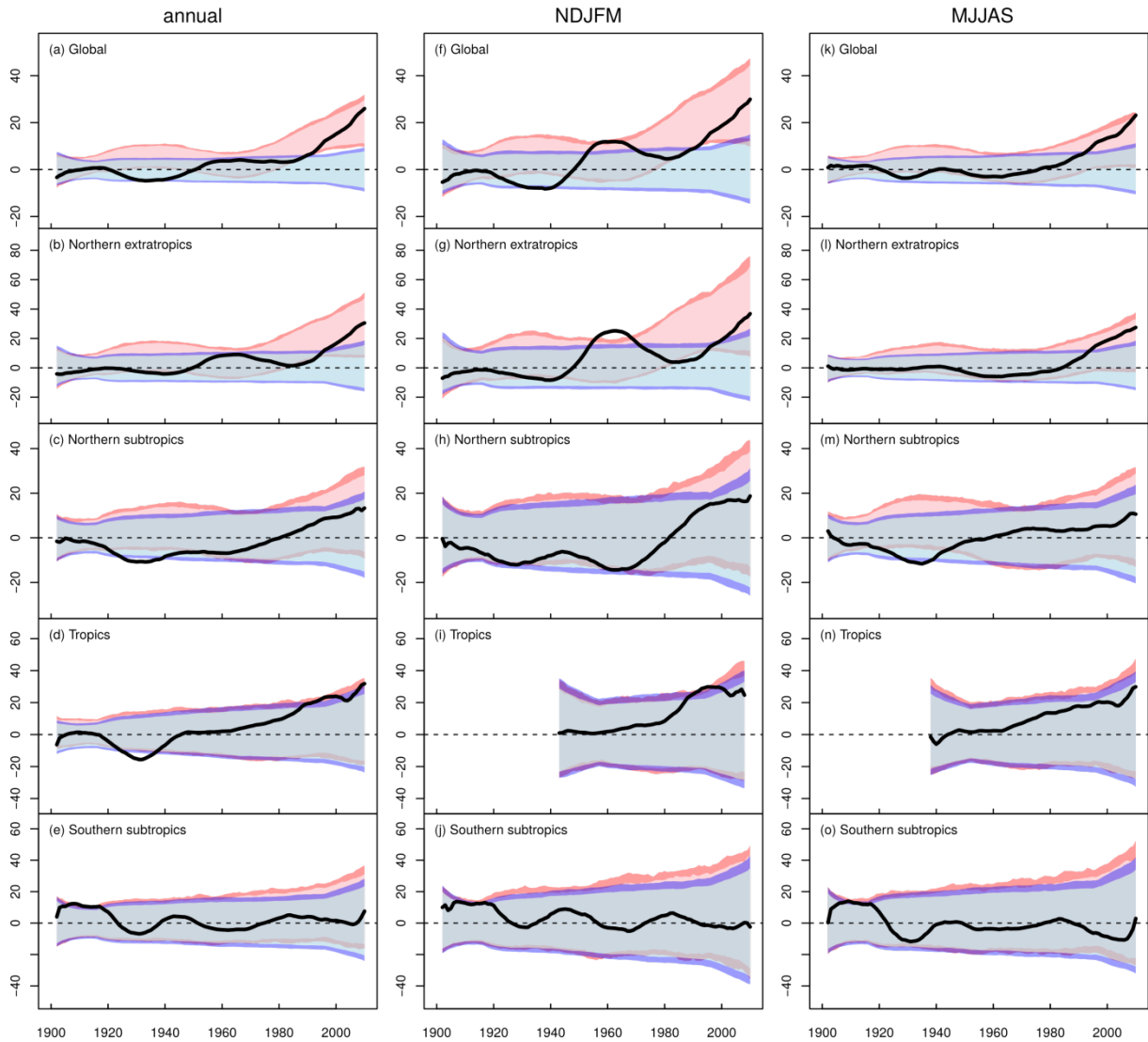
Fig. 3 Long-term non-linear trends in annual record-breaking anomaly (black line) shown (a) globally and for (b) northern extratropics, (c) northern subtropics, (d) tropics, and (e) southern subtropics. The shaded areas reflect the 90% (light shading) and 95% (dark shading) confidence interval derived from long-term non-linear trends of the iid-model (blue color) and Clausius-Clapeyron model (red color). (f)-(j) and (k)-(o) are the same as (a)-(e), respectively, but for seasonal record-breaking anomalies representing NDJFM (middle panel) and MJJAS (right panel).

Clausius-Clapeyron model projects an increase in record-breaking anomaly in the northern extratropics but only little change in the tropics.

In the tropics we instead find indications for super Clausius-Clapeyron scaling, i.e. that record-breaking rainfall increases at a higher rate than expected by the Clausius-Clapeyron

11

relation. Accordingly, the observed record-breaking anomaly shows an increase that reaches the upper end of the 95% confidence level of the Clausius-Clapeyron model. Over the southern subtropics the Clausius-Clapeyron model shows little trend consistent with the observations.

The Clausius-Clapeyron model predicts larger trends for boreal winter (Fig. 3f, g, h) compared to boreal summer (Fig. 3k, l, m). This is explained by the trend-to-variability ratio and follows the same argumentation as given for the comparison between the northern extratropics and the tropics: The larger thermal induced trend in boreal summer is counter acted by the up-to three times larger year-to-year variability in its Rx1day time series.

4   Regional analysis of recent past (1981-2010)

The most distinct feature of the global record-breaking anomaly is a robust increase over the last 30 years. However, we showed that this trend is differently expressed across the latitudes. We therefore analyze the time period 1981-2010 in more detail on a smaller regional scale using a spatial division of the land area similar to that in Field et al. [2012] (table S1 in SI).

Time-averaged record-breaking anomalies between 1981 and 2010 show distinct regional patterns. While the record-breaking anomaly is positive globally and over all latitudinal belts (see bottom panels of Fig. 4), it is more diverse regionally with values ranging from -27% (Mediterranean) to +56% (South East Asia). The box panels in the map of Fig. 4 show the regional mean record-breaking anomaly (+ symbol) with confidence intervals of the iid-model (blue bars) and Clausius-Clapeyron model (red bars). On a global scale, the mean record-breaking anomaly has significantly increased to +12% more rainfall extremes compared to iid-expected in 1980-2010. Significant increases are also found over the northern extra-/subtropics and tropics (see bottom panels of Fig. 4). The magnitude of the increase is largest for the tropics (+18%) and moderate for the northern extra-/subtropics (+12%, +9%). Consistent with this, most subcontinental regions also show an increased record-breaking anomaly over the last 30 years. Significant increases can be found over Central North America (+24%), Europe (+31%), Northern Asia (+21%), the Tibetan Plateau (+31%), and South East Asia (+56%). Some regions show exceptionally high increases in record-breaking anomalies (e.g. South-East Asia) which reach the upper 95% confidence limits of the Clausius-Clapeyron model. Conversely, also significant negative record-breaking anomalies are found, notably in the Mediterranean region (-27%) and Western North America (-21%).
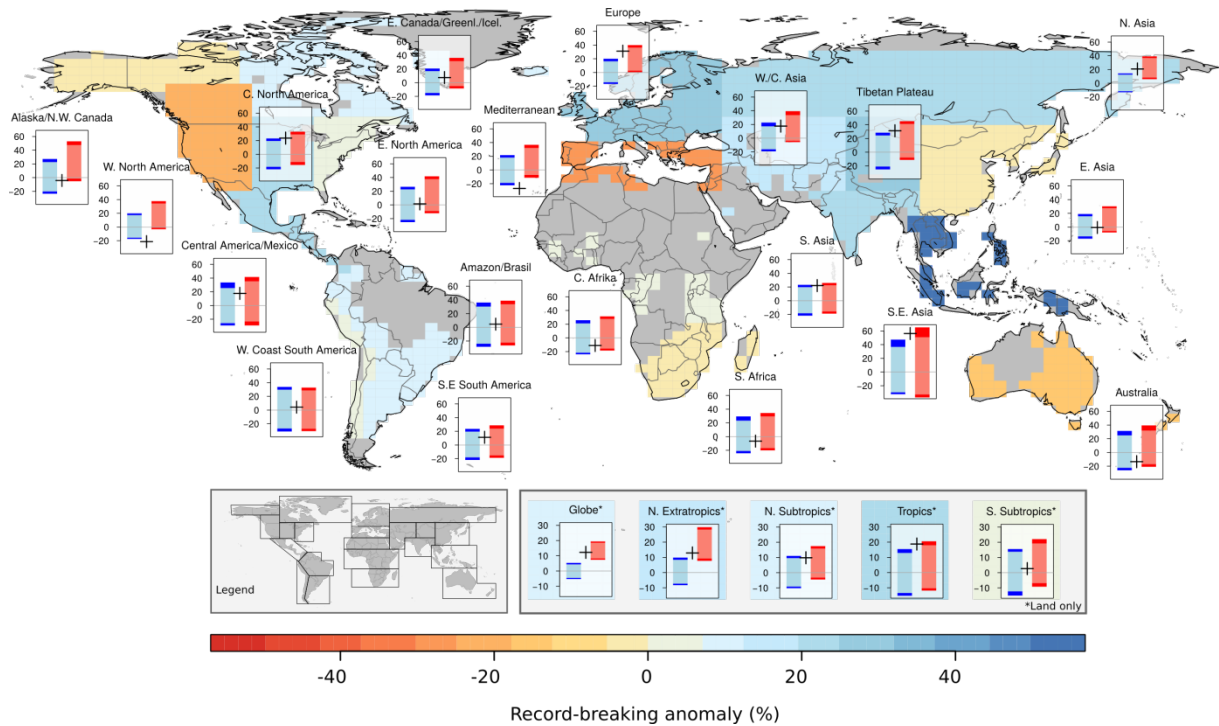
Fig. 4 Annual observed record-breaking anomaly between 1981 and 2010. The magnitude is indicated by different colors at grid cells which contributed to the regional record-breaking anomaly. For each region a separate diagram is shown which includes the observed record-breaking anomaly (+ symbol) and the 90% and 95% confidence interval estimates from the iid-model (blue bars) and the Clausius-Clapeyron model (red bars). Lower panels show the same results for the global mean and the four latitudinal belts (same regions as in Fig. 2-3).

The Clausius-Clapeyron model projects an increase in record-breaking anomaly compared to the iid-model for all regions as all regions have warmed. Thus, significant decreases as found in Western North America and the Mediterranean region cannot be explained by this model. However, for all regions with significant increases in record-breaking anomaly the Clausius-Clapeyron model is able to capture this increase. Regional record-breaking anomalies for 1980-2010 during NDJFM are similar to those for the full year. The largest exception exists for Southern Africa, which exhibits a record-breaking anomaly of +30% during NDJFM compared to -7% for the full year. In addition, the decrease in record-breaking anomaly over the Mediterranean region is more pronounced during NDJFM (-36%) than for the full year (-27%). South East Asia experienced a higher record-breaking anomaly during NDJFM (+80%) than during the full year (+56%). Some regions in the tropics do not provide results for the seasonal record-breaking anomaly due to lack of data (Fig. 5a, b).
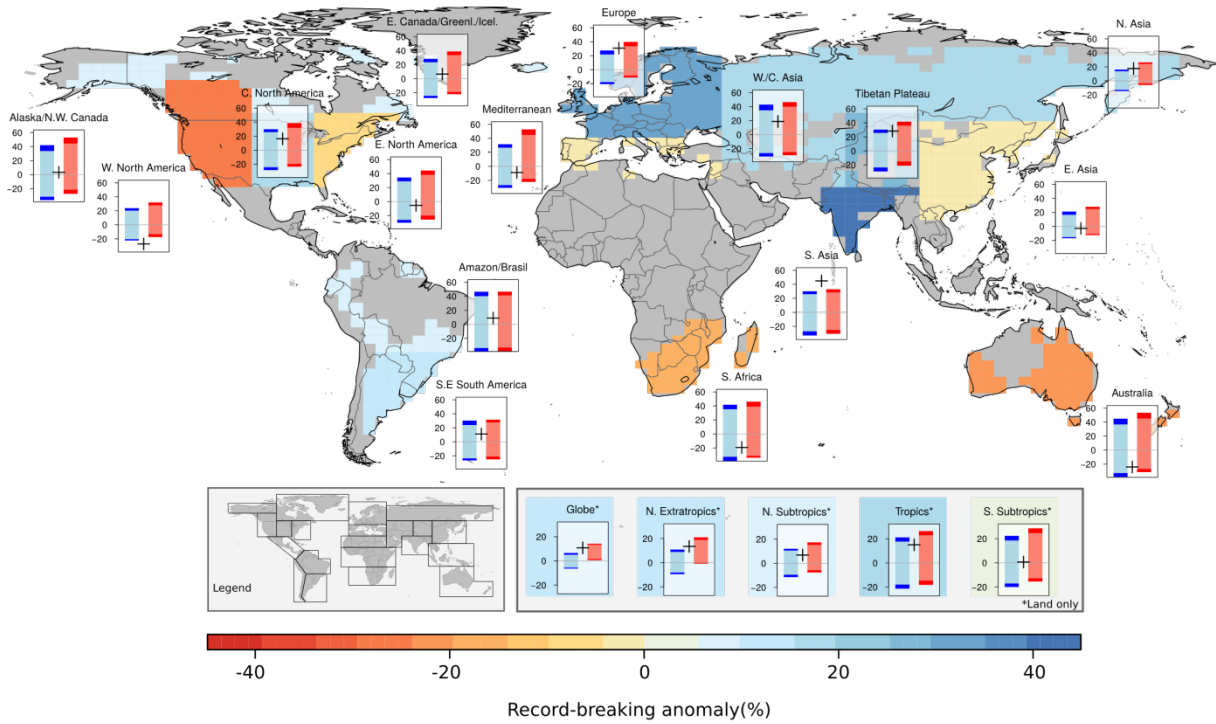
13
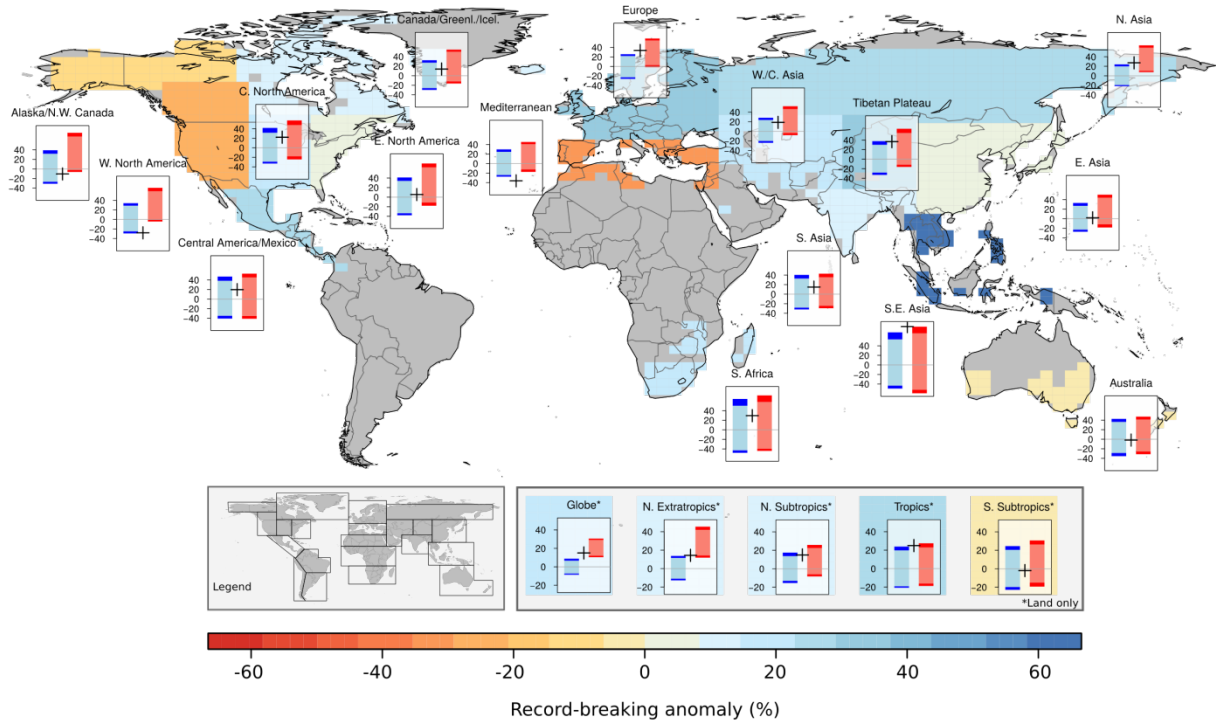
Fig. 5 Same as in Fig. 4, but for record-breaking anomalies during (a) NDJFM and (b) MJJAS.

Results for MJJAS are qualitatively similar. Notable differences only exist for Southern Asia, Australia, and the Mediterranean region. Over Southern Asia, the increase in record-breaking anomaly is significant and about three times larger in MJJAS (+45%) compared to NDJFM (+15%, not significant). Over Australia the decrease in record-breaking anomaly is much larger during winter (MJJAS, -24%) than during summer (NDJFM, -2%). Similarly, in the Mediterranean the decrease in record-breaking anomaly is only significant during winter (NDJFM, -36%), but not during summer (MJJAS, -9%). On a global scale, the 1981-2010 record-breaking anomaly increases significantly in both seasons, i.e. +15% during NDJFM and +11% during MJJAS.

5   Relation with ENSO

One major contributor to natural variability in precipitation patterns is the interplay between El Niño and La Niña events [*Hurrell*, 1995; *Dai and Wigley*, 2000; *Trenberth et al.*, 2003]. In the Southern Hemisphere, a clear spatial pattern of the correlation between the year-to-year variability of the record-breaking anomaly and ENSO (represented by the nino3.4 index) is observed (Fig. 6). Over South East Asia and Australia we see a significant anti-correlation during all seasons implying that these regions experience significantly more record-breaking rainfall during La Niña events than during El Niño. The opposite pattern can be seen over Central and South America. Here, El Niño results in more record-breaking rainfall compared to La Niña events.

In the Northern Hemisphere a separation can be seen over North America with the western areas (Central and Western North America and Alaska) exhibiting more record-breaking rainfall during El Niño events and the eastern regions (East North America, East Canada, and Greenland) experiencing more record-breaking events during La Niña. However, regressions are not significant in most cases. Significant results are found over central west Asia and over the Tibetan Plateau, both of which show a positive correlation between ENSO and record-breaking anomaly.

Over the latitudinal belts, correlations between record-breaking anomaly and ESNO are less obvious (bottom box in Fig. 6). This is due to the fact that regressions with opposite signs in different regions can cancel each other out, as e.g. in the southern subtropics. Nevertheless, rainfall in the Northern Hemisphere (and especially in the subtropics) tends to be intensified during El Niño years leading to a surplus of record-breaking rainfall events.
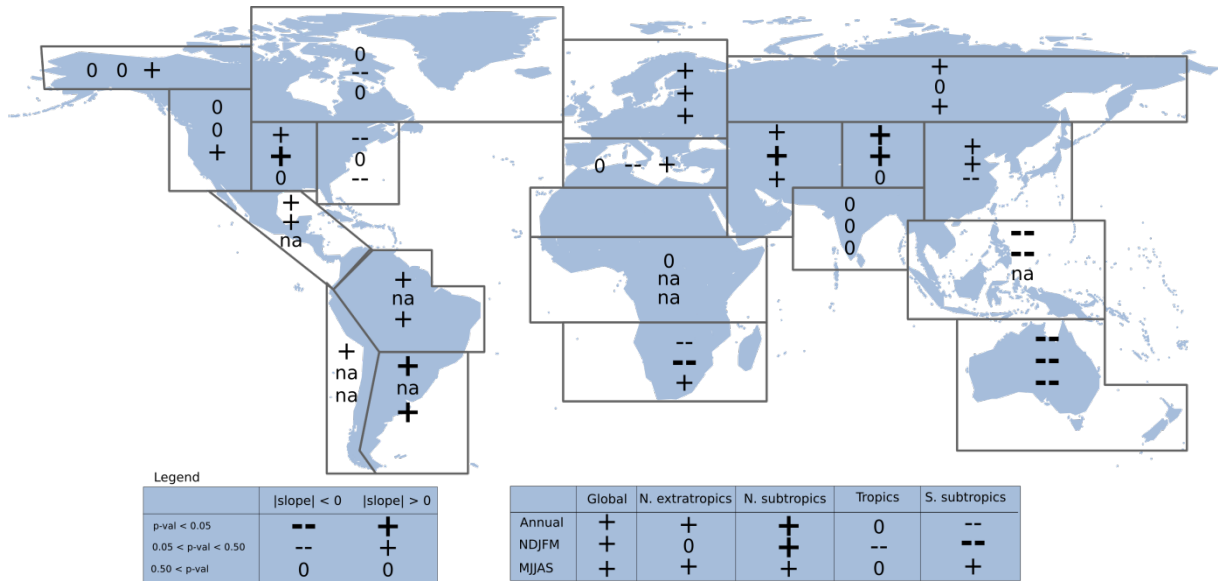
15

Legend

	|slope| < 0	|slope| > 0
p-val < 0.05	--	+
0.05 < p-val < 0.50	--	+
0.50 < p-val	0	0

	Global	N. extratropics	N. subtropics	Tropics	S. subtropics
Annual	+	+	+	0	--
NDJFM	+	0	+	--	--
MJJAS	+	+	+	0	+

Fig. 6 Correlation between the year-to-year variability of the record-breaking anomaly and ENSO represented by the nino3.4 index. For each region and season symbols indicate the sign and strength of the correlation with the "+" symbol indicating more records during El Niño compared to La Niña years and vice versa for the "-" symbol (see legend for details).

6   Summary and discussion

The number of record-breaking rainfall events between 1901 and 2010 is investigated using observations from the HadEX2 data set. We find an increase of +12% in the globally aggregated number of record-breaking rainfall events compared to that expected in a stationary climate over the time period 1981 to 2010. This implies that over the last 30 years, roughly one in ten record-breaking events would not have occurred without climate change. The increase in record-breaking anomaly peaks in 2010 with +88% more record-breaking events than expected in a climate with no long-term change. We show that the long-term increase in record-breaking anomaly cannot be explained by (multi-decadal) natural variability alone but that it is consistent with what would be expected from rising temperatures.

A large and consistent increase in the long-term trend of the record-breaking anomaly since the 1980s is found over the northern extratropics (+37%/+27% in 2010), the tropics (+25%/+30% in 2010), and partly over the northern subtropics (+19%/+11% in 2010), independent of the season (NDJFM/MJJAS). Over the southern subtropics the long-term record-breaking anomaly shows no trend.

On a regional scale the mean record-breaking anomalies between 1981 and 2010 are more diverse and in some cases in the opposite direction. For example, Australia experiences a decline in the number of record-breaking rainfall of -24% (during winter season) at the same time as the record-breaking anomaly over South East Asia increases by +80% (during summer season). Our results support previous findings [*Seneviratne et al.*, 2012], but some new insights are also obtained. For example, we find a significant decrease in the winter record-breaking anomaly over the Mediterranean region. So far, there has only been low confidence about changes in extreme precipitation in this region due to inconsistent trends within domains and across studies [*Kiktev et al.*, 2003; *Caballero*, 2005; *Alexander et al.*, 2006; *García et al.*, 2007; *Pavan et al.*, 2008]. Confidence has also been low for the Asian continent in general except for Western Asia where medium confidence exists for an increase in extreme precipitation confirming our results [*Kwarteng et al.*, 2009; *Rahimzadeh et al.*, 2009]. However, we also find significant results for other Asian regions, i.e. significant increases in record-breaking rainfall over Northern Asia, the Tibetan Plateau, India and South East Asia.

Further, we show that thermally driven moisture increase has significantly contributed to the intensification of extreme rainfalls since the 1980s. In particular, the number of record-breaking events in the last three decades is quantitatively consistent with those projected by the Clausius-Clapeyron model. This model assumes that changes in extreme rainfall intensities scale with temperature changes as given by the Clausius-Clapeyron equation, implying that the maximum moisture in the atmosphere limits the intensity of rainfall extremes. Observations and model results agree best over the northern mid-latitudes and northern subtropics. Conversely, over the tropics, the observed record-breaking anomaly is at the upper end of the 95% range for the Clausius-Clapeyron model, indicating that, here, a super Clausius-Clapeyron scaling is required to explain the observed changes in record-breaking rainfall. This is not unreasonable given that the composition of precipitation types is different between the tropics and sub-/extratropics. Whilst in the tropics daily precipitation is largely convective it can be a mixture of convective and stratiform in the sub-/extratropics. Stratiform precipitation extremes increase with temperature at approximately the Clausius-Clapeyron rate whereas the intensity of convective rainfall tends to be more sensitive to temperature changes and can thus exceed the Clausius-Clapeyron rate [*Berg et al.*, 2013]. Our results indicate that thermodynamics are able to explain much of the observed increase in the record-breaking rainfall which cannot be related to natural climate variability. However, other

factors such as changes in dynamics which were not addressed in this study likely also play a role.

On a regional scale we find examples of decreasing record-breaking anomalies which cannot be attributed to either natural climate variability or to changes in atmospheric moisture content. One example is the negative Mediterranean record-breaking anomaly in winter between 1981 and 2010 which is significant at the 5% confidence level and also well outside the confidence range of the Clausius-Clapeyron model. Hoerling et al. [2012] analyzed Mediterranean rainfall in detail showing that the drying is likely related to changes in sea surface temperature through external radiative forcing.

Results from the linear regression analysis suggest that over some regions the number of record-breaking events is strongly influenced by the ENSO cycle. In particular, we find that South East Asia and Australia exhibit significantly more record-breaking rainfall events during La Niña years, whilst the correlation is reversed for South America, the Tibetan Plateau and the adjacent region of Western Asia. This is in good agreement with results for global patterns of ENSO-induced precipitation shown by Dai et al. [2000].

We argue that the multi-decadal variability of the record-breaking anomaly can partly be explained by the multi-decadal variability in the ENSO cycle. In particular, the drop in the global record-breaking anomaly between 1920 and 1950 as well as the increase during 1950-1980 coincide with years of strong La Niña and El Niño years, respectively (Fig. S14). This is consistent with the positive correlation we find for the global record-breaking anomaly and ENSO. However, over the last 30 years natural climate variability (and in particular ENSO) cannot explain the large and consistent increase in record-breaking anomaly. Instead, over this period, changes in temperature seem to have favored the increased number of record-breaking precipitation events globally.

References

Alexander, L. V. et al. (2006), Global observed changes in daily climate extremes of temperature and precipitation, J. Geophys. Res., 111(D5), D05109, doi:10.1029/2005JD006290.

Allen, M. (1997), Optimal filtering in singular spectrum analysis, Phys. Lett. A, 234(October), 419–428, doi:10.1016/S0375-9601(97)00559-8.

Anderson, A., and A. Kostinski (2011), Evolution and Distribution of Record-Breaking High and Low Monthly Mean Temperatures, J. Appl. Meteorol. Climatol., 50(9), 1859–1871, doi:10.1175/JAMC-D-10-05025.1.

Benestad, R. (2003), How often can we expect a record event?, Clim. Res., 25, 3–13.

Benestad, R. E. (2004), Record-values , non-stationarity tests and extreme value distributions, Glob. Planet. Change, 44(1-4), 11–26.

Benestad, R. E. (2013), Association between trends in daily rainfall percentiles and the global mean temperature, J. Geophys. Res. Atmos., 118(19), 10,802–10,810, doi:10.1002/jgrd.50814.

Berg, P., C. Moseley, and J. O. Haerter (2013), Strong increase in convective precipitation in response to higher temperatures, Nat. Geosci., 6(3), 181–185, doi:10.1038/ngeo1731.

Caballero, R. (2005), The dynamic range of poleward energy transport in an atmospheric general circulation model, Geophys. Res. Lett., 32(2), L02705, doi:10.1029/2004GL021581.

Coumou, D., and S. Rahmstorf (2012), A decade of weather extremes, Nat. Clim. Chang., 2, 491–496, doi:10.1038/nclimate1452.

Coumou, D., A. Robinson, and S. Rahmstorf (2013), Global increase in record-breaking monthly-mean temperatures, Clim. Change, 118(3-4), 771–782, doi:10.1007/s10584-012-0668-1.

Dai, A., and T. Wigley (2000), Global patterns of ENSO-induced precipitation, Geophys. Res. Lett., 27(9), 1283–1286.

Donat, M. G., L. V. Alexander, H. Yang, I. Durre, R. Vose, and J. Caesar (2013a), Global Land-Based Datasets for Monitoring Climatic Extremes, Bull. Am. Meteorol. Soc., 94(7), 997–1006, doi:10.1175/BAMS-D-12-00109.1.

Donat, M. G. et al. (2013b), Updated analyses of temperature and precipitation extreme indices since the beginning of the twentieth century: The HadEX2 dataset, J. Geophys. Res. Atmos., 118(5), 2098–2118, doi:10.1002/jgrd.50150.

Field, C. B., V. Barros, T. F. Stocker, and Q. Dahe (2012), Managing the Risks of Extreme Events and Disasters to Advance Climate Change Adaptation, edited by C. B. Field, V. Barros, T. F. Stocker, and Q. Dahe, Cambridge University Press, Cambridge.

Frei, C., and C. Schär (2001), Detection Probability of Trends in Rare Events: Theory and Application to Heavy Precipitation in the Alpine Region, J. Clim., 14(7), 1568–1584, doi:10.1175/1520-0442(2001)014<1568:DPOTIR>2.0.CO;2.

García, J., M. C. Gallego, A. Serrano, and J. Vaquero (2007), Trends in Block-Seasonal Extreme Rainfall over the Iberian Peninsula in the Second Half of the Twentieth Century, J. Clim., 20(1), 113–130, doi:10.1175/JCLI3995.1.

Golyandina, N., V. V. Nekrutkin, and A. A. Zhigljavsky (2001), Analysis of Time Series Structure: SSA and Related Techniques.

Harris, I., P. D. Jones, T. J. Osborn, and D. H. Lister (2014), Updated high-resolution grids of monthly climatic observations - the CRU TS3.10 Dataset, Int. J. Climatol., 34(3), 623–642, doi:10.1002/joc.3711.

Hawcroft, M. K., L. C. Shaffrey, K. I. Hodges, and H. F. Dacre (2012), How much Northern Hemisphere precipitation is associated with extratropical cyclones?, Geophys. Res. Lett., 39(24), L24809, doi:10.1029/2012GL053866.

Hoerling, M., J. Eischeid, J. Perlwitz, X. Quan, T. Zhang, and P. Pegion (2012), On the Increased Frequency of Mediterranean Drought, J. Clim., 25(6), 2146–2161, doi:10.1175/JCLI-D-11-00296.1.

Hurrell, J. W. (1995), Decadal trends in the north atlantic oscillation: regional temperatures and precipitation., Science, 269(24), 676–679, doi:10.1126/science.269.5224.676.

Kharin, V. V., F. W. Zwiers, X. Zhang, and G. C. Hegerl (2007), Changes in Temperature and Precipitation Extremes in the IPCC Ensemble of Global Coupled Model Simulations, J. Clim., 20(8), 1419–1444, doi:10.1175/JCLI4066.1.

Kiktev, D., D. M. H. Sexton, L. Alexander, and C. K. Folland (2003), Comparison of Modeled and Observed Trends in Indices of Daily Climate Extremes, J. Clim., 16(22), 3560–3571, doi:10.1175/1520-0442(2003)016<3560:COMAOT>2.0.CO;2.

Kiktev, D., J. Caesar, L. V. Alexander, H. Shiogama, and M. Collier (2007), Comparison of observed and multimodeled trends in annual extremes of temperature and precipitation, Geophys. Res. Lett., 34(April), 2–6, doi:10.1029/2007GL029539.

Kwarteng, A. Y., S. Dorvlo, and G. T. Vijaya (2009), Analysis of a 27-year rainfall data (1977 – 2003) in the Sultanate of Oman, , 617(July 2008), 605–617, doi:10.1002/joc.

Meehl, G. a., C. Tebaldi, G. Walton, D. Easterling, and L. McDaniel (2009), Relative increase of record high maximum temperatures compared to record low minimum temperatures in the U.S., Geophys. Res. Lett., 36(December), 1–5, doi:10.1029/2009GL040736.

Min, S.-K., X. Zhang, F. W. Zwiers, and G. C. Hegerl (2011), Human contribution to more-intense precipitation extremes., Nature, 470(7334), 378–81, doi:10.1038/nature09763.

NOAA National Climatic Data Center (2010), State of the Climate: Global Analysis for Annual 2010, Publ. online December 2010, (July 2009), http://www.ncdc.noaa.gov/sotc/global/2010/13.

Pall, P., M. R. Allen, and D. a. Stone (2007), Testing the Clausius–Clapeyron constraint on changes in extreme precipitation under CO2 warming, Clim. Dyn., 28(4), 351–363, doi:10.1007/s00382-006-0180-2.

Pavan, V., R. Tomozeiu, C. Cacciamani, and M. Di Lorenzo (2008), Daily precipitation observations over Emilia-Romagna: mean values and extremes, Int. J. Climatol., 28(15), 2065–2079, doi:10.1002/joc.1694.

Rahimzadeh, F., A. Asgari, and E. Fattahi (2009), Variability of extreme temperature and precipitation in Iran during recent decades, , 343(August 2008), 329–343, doi:10.1002/joc.

Rahmstorf, S., and D. Coumou (2011), Increase of extreme events in a warming world., Proc. Natl. Acad. Sci. U. S. A., 108(44), 17905–9, doi:10.1073/pnas.1101766108.

Redner, S., and M. R. Petersen (2005), On the Role of Global Warming on the Statistics of Record-Breaking Temperatures, Phys. Rev. E, 11, doi:10.1103/PhysRevE.74.061114.

Rogers, J. C. (1985), Atmospheric Circulation Changes Associated with the Warming over the Northern North Atlantic in the 1920s, J. Clim. Appl. Meteorol., 24(12), 1303–1310, doi:10.1175/1520-0450(1985)024<1303:ACCAWT>2.0.CO;2.

Scaife, A. a. et al. (2011), Climate change projections and stratosphere–troposphere interaction, Clim. Dyn., 38(9-10), 2089–2097, doi:10.1007/s00382-011-1080-7.

Seneviratne, S. I. et al. (2012), Changes in climate extremes and their impacts on the natural physical environment, in Managing the Risks of Extreme Events and Disasters to Advance Climate Change Adaptation, edited by C. B. Field et al., pp. 109–230, Cambridge University Press.

Shiu, C.-J., S. C. Liu, C. Fu, A. Dai, and Y. Sun (2012), How much do precipitation extremes change in a warming climate?, Geophys. Res. Lett., 39(17), doi:10.1029/2012GL052762.

Singh, M. S., and P. a. O'Gorman (2014), Influence of microphysics on the scaling of precipitation extremes with temperature, Geophys. Res. Lett., doi:10.1002/2014GL061222.

Trenberth, K. (2011), Changes in precipitation with climate change, Clim. Res., 47(1), 123–138, doi:10.3354/cr00953.

Trenberth, K. E. (2012), Framing the way to relate climate extremes to climate change, Clim. Change, doi:10.1007/s10584-012-0441-5.

Trenberth, K. E., A. Dai, R. M. Rasmussen, and D. B. Parsons (2003), The changing character of precipitation, Bull. Am. Meteorol. Soc., 84(September), 1205–1217+1161, doi:10.1175/BAMS-84-9-1205.

Trenberth, K. E. et al. (2007), Obervations: Surface and Atmospheric Climate Change, in Climate Change 2007: The Physical Sience Basis, edited by S. Solomon, Q. Dahe, M. R. Manning, Z. Chen, M. Marquis, K. B. Averyt, M. Tignor, and H. L. Miller, Cambridge University Press, Cambridge, UK, and New York, NY, USA.

Westra, S., L. V. Alexander, and F. W. Zwiers (2013), Global Increasing Trends in Annual Maximum Daily Precipitation, J. Clim., 26(11), 3904–3918, doi:10.1175/JCLI-D-12-00502.1.

Wilks, D. S. (1997), Resampling hypothesis tests for autocorrelated fields, J. Clim., 10, 65–82, doi:10.1175/1520-0442(1997)010<0065:RHTFAF>2.0.CO;2.

Zhang, X., F. W. Zwiers, G. C. Hegerl, F. H. Lambert, N. P. Gillett, S. Solomon, P. a Stott, and T. Nozawa (2007), Detection of human influence on twentieth-century precipitation trends., Nature, 448(7152), 461–5, doi:10.1038/nature06025.

Zhang, X., H. Wan, F. W. Zwiers, G. C. Hegerl, and S.-K. Min (2013), Attributing intensification of precipitation extremes to human influence, Geophys. Res. Lett., 40(19), 5252–5257, doi:10.1002/grl.51010.